Impact of Deposit Ageing on Thermal Fouling: Lumped Parameter Model

Edward. M. Ishiyama
Dept. of Chemical Engineering and Biotechnology, University of Cambridge, New Museums Site, Cambridge CB2 3RA, U.K.

Francesco Coletti and Sandro Macchietto
Dept. of Chemical Engineering and Chemical Technology, Imperial College London, South Kensington Campus, London SW7 2AZ, U.K.

W.R. Paterson and D. I. Wilson
Dept. of Chemical Engineering and Biotechnology, University of Cambridge, New Museums Site, Cambridge CB2 3RA, U.K.

DOI 10.1002/aic.11978
Published online August 24, 2009 in Wiley InterScience (www.interscience.wiley.com).

The thermal and hydraulic performance of heat exchangers can be seriously impaired by the formation of fouling deposits on the heat transfer surfaces. The thermal effect of fouling can be complicated when the deposit is subject to ageing, represented here as a change in deposit thermal conductivity (but not thickness) over time. In this article, we revisit the ageing concept for crude oil fouling proposed by Nelson (Refiner Nat Gas Manufacturer. 1934;13:271–276, 292–298), using a numerical model incorporating first order kinetics to generate quantitative comparisons of different ageing rates. Results are reported for lumped parameter systems (which also simulate point measurement methods commonly used in laboratory testing) that demonstrate that ageing can have a substantial influence on the rate of heat transfer and hence on the surface temperature and rate of fouling. Rapid ageing (compared with the rate of deposition) does not pose problems, but slow ageing, or the use of constant heat fluxes in experiments, can lead to modified thermal fouling behavior. It is concluded that deposit ageing dynamics should be considered alongside deposition rate dynamics when interpreting experimental fouling data and when modeling fouling behavior in support of heat exchanger design or operation. © 2009 American Institute of Chemical Engineers
AIChE J, 56: 531–545, 2010
Keywords: Crude oil, heat exchanger, fouling, ageing

Introduction

The formation of fouling deposits on heat transfer surfaces reduces overall heat transfer coefficients and usually increases the pressure drop across heat exchangers via increases in surface friction and/or reduction in flow area. Fouling may still be 'the major unsolved problem in heat transfer' as identified by Taborek et al.,[1] and remains a major problem in many processes. The importance of fouling mitigation has grown with the increasing importance of factors such as energy prices and the environmental impacts of energy inefficiency, e.g., carbon dioxide emissions. Heat exchanger fouling in general is a major economic problem, accounting for 0.25% of the gross national product (GNP) in

Correspondence concerning this article should be addressed to D. I. Wilson at diw11@cam.ac.uk

© 2009 American Institute of Chemical Engineers

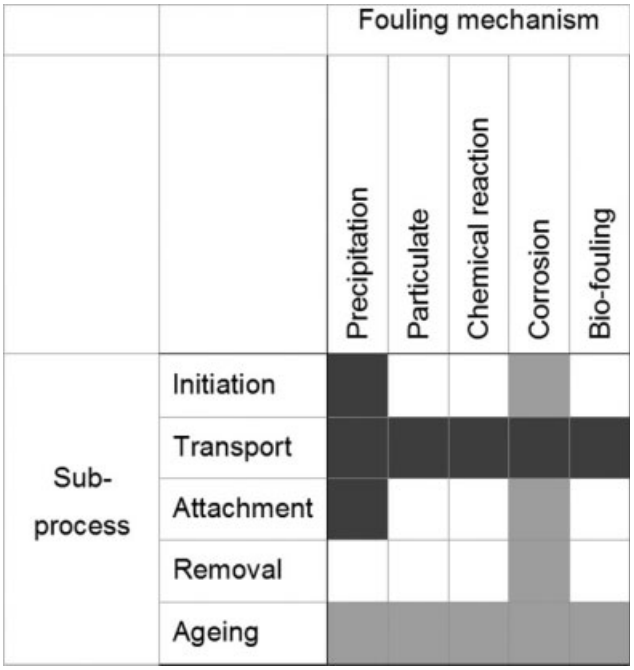

Figure 1. 5×5 fouling matrix (after Epstein,[3] 1983).

Dark shading indicates areas where research had focused: grey areas where little research had been done.

the highly industrialized countries.[2] Epstein reviewed the current understanding of fouling in 1983 and presented his conclusions in a 5 × 5 matrix, which is reproduced as Figure 1.[3] This classification of fouling by mechanisms and stages has been widely followed. More recent reviews have reported progress in understanding the stages in fouling in all but the final, ageing, step.[4]

'Ageing' refers to the modification of the fouling deposit after the material has been incorporated as a surface layer. The change in deposit hardness, or in thermal conductivity, can have significant effects on subsequent fouling and therefore on process performance. Chew et al.[5] highlighted the role of ageing in cleaning, as ageing ultimately dictates the nature of the material to be removed in such operations.

Ageing has received relatively little attention to date, even though Nelson proposed a semi-quantitative model for fouling involving ageing in crude oil furnaces in 1934.[6] He considered the formation of coke (carbonaceous fouling layer) at the high temperatures found in furnaces, where vaporization results in the oil being present as an annular film at the tube wall. He described coke formation (fouling) as arising from chemical reaction in this film and calculated the impact on heat transfer. He noted that the properties of the layer would change with temperature and time, essentially baking, and reported values of thermal conductivities of different carbonaceous materials for comparison. Atkins (1962) considered fouling in furnaces and the hottest exchangers in a preheat train, and proposed that the formation of the hard coke fouling layer occurred via two steps, namely the deposition of a porous coke or tarry layer which was then converted to a hard coke layer.[7] The transition from the tarry or porous layer to the hard coke was modeled as according at a fixed temperature, so that the growth of a hard coke followed a moving front.

Crittenden and Kolaczkowski[8] extended the Atkins two-layer concept, which they modeled as

$$\text{Precursors (in bulk fluid)} \xrightarrow{\text{deposition}} \text{tarry foulant layer } (\delta_{\text{tar}}, \lambda_{\text{tar}}) \xrightarrow{\text{ageing}} \text{coke } (\delta_{\text{coke}}, \lambda_{\text{coke}})$$

where δ and λ refer to the thickness and thermal conductivity of each layer, respectively. They generated a quantitative description of the evolution of the overall fouling resistance, in which they accounted for the changing thicknesses of the tarry layer and its conversion to the coke layer. The growth of tarry layer was described as a competition between deposition, mass transfer of tarry components back into the bulk solution, and shear removal of the tarry layer. The ageing (conversion) step was modeled as being first order in tarry layer component concentration and following an Arrhenius-type temperature dependency. They compared the trends predicted by their model with chemical reaction fouling data reported by Watkinson and Epstein,[9] where the deposit was described as 'soot-like', so were not able to explore the coke formation regime.

Ageing has been studied in some detail for crystallization fouling (e.g., calcium sulphate fouling in heat exchangers[10]) but the area where it has received particular attention is in wax deposition in undersea oil pipelines.[11–15] In both cases, ageing causes hardening of the deposits and makes their removal more difficult. In the latter case, the impact on heat transfer is not large because the thermal conductivity of the solid phase is similar to that of the oil phase, whereas in preheat train (PHT) crude oil fouling the thermal conductivity can change by almost an order of magnitude.

According to Watkinson,[16] the thermal conductivity of oils lies in the range 0.1–0.2 W m^{-1} K^{-1}, whereas that of hardened and coke-like deposits has been reported to lie in the range 0.5–1.0 W m^{-1} K^{-1}. The limiting value for a coke deposit may be compared with that of amorphous graphitic carbon, at ~2 W m^{-1} K^{-1},[17] although Kern[18] reported thermal conductivity values of petroleum coke of 5 W m^{-1} K^{-1} at 500°C and 5.8 W m^{-1} K^{-1} at 100°C. The thermal conductivity ultimately depends on the ratios of different carbon allotropes present in coke. The chemistry responsible for ageing in crude oil deposits is poorly understood, partly due to the variation in composition between crudes and the associated range in reaction pathways available.

This article addresses the impact of ageing on the thermal effects of fouling, with particular reference to crude oil refinery applications. The impact of changes in thermal conductivity can be illustrated as follows. Consider the commonly used definition of thermal fouling resistance in process heat transfer, R_f, viz.

$$\frac{1}{U} = \frac{1}{U_{\text{cl}}} + R_{\text{f}} \tag{1}$$

where U is the overall heat transfer coefficient and 'cl' refers to deposit-free operation. This commonly used method for obtaining the overall fouling resistance from an operating

shell-and-tube heat exchanger is prone to systematic error when the effects of shell-side by-passing, and the effect of logarithmic mean temperature difference on overall heat transfer coefficient, are neglected (e.g., Jeronimo et al.[19] and Takemoto et al.[20]). These considerations notwithstanding, Eq. 1 is used here as a reasonable and illustrative representation of the overall heat transfer coefficient.

Consider a thin slab of fouling deposit of thermal conductivity λ_f and thickness δ: Yeap et al.[21] showed that the thermal resistance can be approximated for most heat exchanger tube applications in crude oil service as

$$R_f = \delta/\lambda_f \tag{2}$$

Combining Eqs. 1 and 2 yields

$$U = \frac{U_{cl}}{1 + U_{cl}R_f} \equiv \frac{U_{cl}}{1 + Bi_f} = \frac{U_{cl}}{1 + U_{cl}\delta/\lambda_f} \tag{3}$$

where Bi_f is the fouling Biot number. For a typical refinery U_{cl} value of 1000 W $m^{-2}K^{-1}$, Eq. 3 indicates that the thickness of deposit required to reduce the heat transfer coefficient by half will change from 0.1 to 0.5 mm if λ_f changes from 0.1 to 0.5 W m^{-1} K^{-1}. The hydraulic impact of fouling (i.e., pressure drop–flow rate relationship) is not affected by this change (there is no evidence to date to suggest that crude fouling deposits shrink on ageing) but the relationship between the hydraulic and thermal effects will change, as demonstrated by Yeap et al. Thermal ageing will, however, affect the temperature at the deposit/crude interface, which is recognized to be a key variable influencing the fouling rate. In our analysis, we will be assuming that the deposition does not affect surface roughness significantly: a brief discussion of roughness effects is given in Appendix A. The methodology for calculating the friction factor and the surface roughness value used are detailed under section titled, 'Modeling of flow and conduction'. When crude is being heated, as in a refinery preheat train, deposit formation will initially decrease the deposit/crude interface temperature. Subsequent ageing—increasing λf—will cause the deposit/crude interface temperature to rise, compared with the case of a nonageing deposit, other things being equal. This will give rise to complex fouling resistance-time behavior, which we demonstrate here can be (indirectly) related to changes in fouling mechanisms.

We present here a simple model for the ageing of crude oil deposits based on simple chemical kinetics, namely first order reaction and Arrhenius temperature dependence. We combine this model with deposition models incorporating temperature and velocity effects (specifically, the 'threshold fouling' formulation reported by Polley et al.[22]) in semi-analytical and numerical simulations of heat transfer in a heat exchanger tube. The analysis yields results with important implications for interpretation of thermal fouling behavior in situations where ageing may occur, such as in the interpretation of plant operating data. We illustrate the concepts with simulations of lumped parameter systems. The results are also applicable to point measurements, such as the data obtained from laboratory fouling tests, which are often operated under conditions of either constant tube-wall temperature or constant heat flux. A new numerical treatment is introduced to illustrate the effect on these two modes of operation.

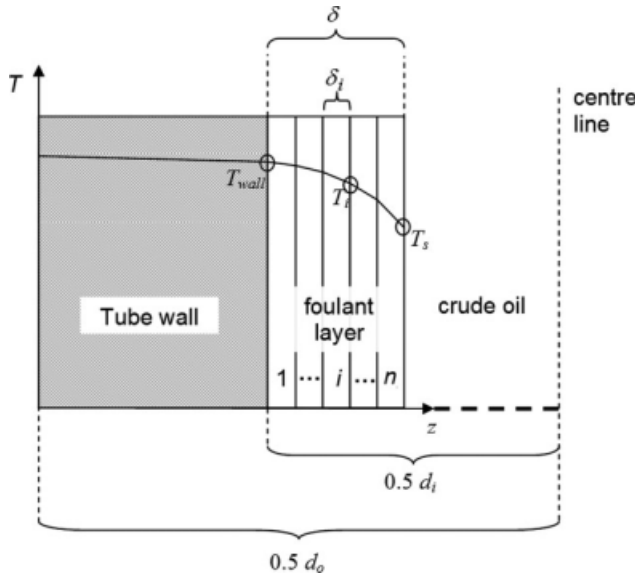

Figure 2. Schematic of foulant layer.

Axis T represent the temperature and z the distance from the tube outer surface, measured towards the tube centre line. Foulant layers are labeled from 1 to n, with n marking fresh deposit at the layer-oil interface. d_i is the tube internal diameter, d_o is the tube external diameter, δ is the total deposit thickness, δ_i is the deposit thickness of the ith layer, T_{wall} is the wall temperature, T_i is the surface temperature of the ith layer (facing the centre line), T_s is the deposit/oil interface temperature.

Model Formulation

Ageing model

We consider, with little loss of generality, the case of a shell-and-tube heat exchanger where a fluid prone to fouling (e.g., crude oil) flows through the tubes and a non-fouling stream flows on the shell side. Fouling deposits are therefore formed only on the tube side. In this article, we consider a lumped parameter model, with no axial distribution and averaged conditions. The deposit is modeled as series of layers, laid down at fixed time steps (in this article, daily) to form a series of annuli with varying history (Figure 2). Once deposited, each layer is simply covered by the next layer, and deposition occurs only at the deposit-oil interface. The thickness of the ith layer is denoted δ_i, and does not change with time after deposition. The thermal conductivity of the ith layer, denoted $\lambda_{f,i}$, however, does increase with time; this is what we mean by ageing.

The upper limit of thermal conductivity, i.e., for fully coked material, is denoted $\lambda^{\infty}_{f,i}$, whereas the freshly deposited foulant always has a thermal conductivity, $\lambda^{0}_{f,i}$ corresponding to the lower bound of the observed range, say 0.2 W m^{-1} K^{-1}. The zero superscript here denotes the initial condition.

Most fouling models describe the effect of deposition in terms of the overall fouling resistance and we assume that such models can be used to calculate the change in deposit thickness, via Eq. 2, for given surface conditions: the thickness of each sub-layer, δ_i, is calculated from

$$\delta_i = \left.\frac{\mathrm{d}\delta}{\mathrm{d}t}\right|_i \cdot \Delta t = \lambda^0_{\mathrm{f},i} \cdot \left(\frac{\mathrm{d}R_{\mathrm{f},s}}{\mathrm{d}t}\right) \cdot \Delta t \tag{4}$$

where $\left.\frac{\mathrm{d}\delta}{\mathrm{d}t}\right|_i$ is the local rate of deposit growth at time period i and Δt the time step over which the deposit forms; $(\frac{\mathrm{d}R_{\mathrm{f},s}}{\mathrm{d}t})$ is the thermal fouling rate at the deposit/oil interface. The thickness of the sub-layer does not change: it is determined by the conditions at its formation. The overall fouling resistance, R_f, after n layers have been formed, is estimated as a series of resistances, (ignoring curvature effects, which would have to be included for a thick deposit, $\delta/d_\mathrm{i} > 0.05$, where d_i is the tube internal diameter):

$$R_\mathrm{f} = \sum_{i=1}^{n} \frac{\delta_i}{\lambda_{\mathrm{f},i}} \tag{5}$$

and the total deposit thickness δ, at time $t = n\Delta t$ (when n layers have been formed) is given by

$$\delta = \sum_{i=1}^{n} \delta_i \tag{6}$$

The thermal conductivity of each foulant layer at time t is assumed to vary between the limiting values $\{\lambda^0_{\mathrm{f},i} \le \lambda^t_{\mathrm{f},i} \le \lambda^\infty_{\mathrm{f},i}\}$ according to the following, simple model:

$$\lambda^t_{\mathrm{f},i} = \lambda^\infty_{\mathrm{f},i} + \left[\lambda^0_{\mathrm{f},i} - \lambda^\infty_{\mathrm{f},i}\right] \cdot y^t_i \tag{7}$$

where y^t_i is named the 'youth' variable:

$$y^0_i = 1 \tag{8a}$$

$$0 \le y^t_i \le 1 \tag{8b}$$

The youth variable is postulated to decline from its initial value of 1 according to a first order kinetic scheme, viz.

$$\frac{\mathrm{d}y^t_i}{\mathrm{d}t} = -k^t_i \cdot y^t_i \tag{9}$$

or

$$\frac{\mathrm{d}\left(\ln y^t_i\right)}{\mathrm{d}t} = -k^t_i \tag{10}$$

where k^t_i is an ageing rate constant and is postulated to follow an Arrhenius dependency on temperature:

$$k^t_i = A \exp\left(\frac{-E_\mathrm{a}}{RT_{i,\mathrm{d}}}\right) \tag{11}$$

where $T_{i,\mathrm{d}}$ is the arithmetic average temperature of the ith deposit layer, A a pre-exponential factor which defines the absolute rate of decay, E_a the activation energy of ageing (determining its temperature dependency), and R the gas constant. The rate of change of thermal conductivity of each layer is therefore dependent on the local temperature, via

$$\frac{\mathrm{d}\ln y^t_i}{\mathrm{d}t} = -A \exp\left(\frac{-E_\mathrm{a}}{RT_{i,\mathrm{d}}}\right) \tag{12}$$

where $T_{\mathrm{i,d}}$ varies with position and time.

This idealized model encompasses the key phenomena, namely an evolution of deposit thermal conductivity between the limiting values, at a rate depending on the local temperature. More elaborate models could be employed, but experimental data would be required to identify the shortcomings in the current formulation. Experimental studies on coker deposits by Fan and Watkinson have demonstrated that ageing is associated with changes in chemical composition as well as weight loss.[23,24] They have also shown that the drop in H/C atomic ratio with the ageing time can be approximately expressed by a first order exponential decay equation. Equation 12 was inferred from the experimental measurements on the effect of ageing on H/C ratio (see Appendix B). However, the effect of ageing on deposit thermophysical properties has yet to be investigated in detail.

The activation energy E_a is a key parameter, but quantitative values are not currently available. If the ageing reaction is endothermic, it is possible to propose a lower limit for the activation energy for ageing.[25] Some information, however, does exist in the area of autoxidative polymerization, where Taylor and Wallace postulated the following overall reaction for the formation of foulant deposit[26–28]:

$$\mathrm{C_{10}H_{24}} + \text{traces of S, N} \xrightarrow{\mathrm{O_2}} \underset{\text{(Soluble oxidation product)}}{\mathrm{C_{10}H_{22}S_{0.3}N_{0.05}O_{1.0}}} \xrightarrow{\mathrm{O_2},\Delta} \underset{\text{(Insoluble polymer, foulant)}}{\mathrm{C_{31}H_{59}S_{0.5}N_{0.5}O_{7.5}}}$$

Taking the insoluble polymers to have similar properties to polyaromatic hydrocarbons, the enthalpies of formation are positive (e.g., anthracene ΔH_f (solid) = 120 kJ/mol[29]; triphenylene ΔH_f (solid) = 141.0 ± 0.5 kJ/mol[30]). These data indicate that the ageing process (polyaromatic to coke) is an exothermic process, rendering the activation energy not readily predictable. In general, therefore, the parameters in the above ageing model will have to be established from regression of experimental data. In the following, realistic ranges are used for the parameter values and a parametric analysis is carried out to show their effect in various typical limit conditions of interest (fast ageing, etc.).

The nonlinear temperature dependency in Eq. 12, when combined with the moving boundary problem set by a growing deposit layer, means that analytical solutions are not readily obtainable so numerical integration is employed here.

Coupling of ageing and deposition processes

The model in the "Ageing model" section describes the fouling process as the deposition of a series of layers which age at different rates, depending on their temperature–time history. The rate of deposition at the fouling layer-fluid interface is rarely constant, however, and is often controlled by the interface temperature, T_s. The evolution of this temperature must be considered, as well as the temperature

dependency of the deposition step. Hence, deposition and ageing are coupled. The purpose of this section is to show how the separate models of deposition and ageing may be combined and yield equations that can be used to model simultaneous deposition and ageing.

Calculation of the interface temperature requires evaluation of the thermal resistance of each deposit layer, which is simplified by the assumption that δ_i does not change with time. Equation 4 then gives

$$\frac{\mathrm{d}R^t_{\mathrm{f},i}}{\mathrm{d}t} = -\frac{\delta_i}{{\lambda^t_{\mathrm{f},i}}^2}\left(\frac{\mathrm{d}\lambda_{\mathrm{f},i}}{\mathrm{d}t}\right) \tag{13}$$

Here, superscript t denotes a time instance. Combining Eqs.7, 11, and 13 gives

$$\frac{\mathrm{d}R^t_{\mathrm{f},i}}{\mathrm{d}t} = A\left[\lambda^0_{\mathrm{f},i} - \lambda^\infty_{\mathrm{f},i}\right]\delta_i \frac{y^t_i}{{\lambda^t_{\mathrm{f},i}}^2}\exp\left(\frac{-E_\mathrm{a}}{RT_{i,\mathrm{d}}}\right) = A^* \frac{y^t_i}{{\lambda^t_{\mathrm{f},i}}^2}\exp\left(\frac{-E_\mathrm{a}}{RT_{i,\mathrm{d}}}\right) \tag{14}$$

where $A^* = A[\lambda^0_{\mathrm{f},i} - \lambda^\infty_{\mathrm{f},i}] \cdot \delta_i$: A^* does not vary over time. Integration of Eq. 14 over time with limits of $R^t_{\mathrm{f},i}$ from $R^{t_{n-1}}_{\mathrm{f},i}$ to $R^{tn}_{\mathrm{f},i}$ and t from $t_{\mathrm{n}-1}$ to t_n (where $\Delta t = t_\mathrm{n} - t_{\mathrm{n}-1}$ is a fixed time interval, in our case one day) yields

$$\int_{R^{t_{n-1}}_{\mathrm{f},i}}^{R^{t_n}_{\mathrm{f},i}} \mathrm{d}R^t_{\mathrm{f},i} = \int_{t_{n-1}}^{t_n} A^* \frac{y^t_i}{{\lambda^t_{\mathrm{f},i}}^2}\exp\left(\frac{-E_\mathrm{a}}{RT_{i,\mathrm{d}}}\right)\mathrm{d}t \tag{15}$$

Solving with Eqs. 2, 7, and 9 gives

$$\frac{R^{t_n}_{\mathrm{f},i}}{\delta_i} = \frac{1}{\lambda^\infty_{\mathrm{f},i}}\left(\frac{X}{1+X}\right)$$

where

$$X = \left(\frac{R^{t_{n-1}}_{\mathrm{f},i}}{\delta_i - \lambda^\infty_{\mathrm{f},i}R^{t_{n-1}}_{\mathrm{f},i}}\right)\exp\left[A\exp\left(-\frac{E_\mathrm{a}}{RT_{i,\mathrm{d}}}\right)\Delta t\right] \tag{16}$$

Equation 16 represents the fouling resistance of the ith layer, $R^{t_n}_{\mathrm{f},i}$, at time t_n as a function of the fouling resistance of the layer in the previous time period, $R^{t_{n-1}}_{\mathrm{f},i}$, and its thickness, δ_i.

A method to calculate δ_i as a function of the conditions at the deposit/fluid interface is therefore needed. Several quantitative fouling rate models exist, varying in form according to the fouling mechanism adopted (e.g., Figure 1, Epstein[3]). We here employ the relationship developed by Polley et al.[22] for tube-side crude oil fouling:

$$\frac{\mathrm{d}R_\mathrm{f}}{\mathrm{d}t} = \max\left\{0, \alpha Re^{-0.8}Pr^{-0.33}\exp\left(-\frac{E_\mathrm{f}}{RT_\mathrm{s}}\right) - \gamma Re^{0.8}\right\} \tag{17}$$

where α and γ are fouling rate constants, E_f is the activation energy of fouling (which may differ from the activation energy of ageing), and T_s is the temperature of the surface, i.e., of the crude-wall or crude-deposit interface. The Reynolds number, Re, is calculated via

$$Re = \frac{u_\mathrm{m}(d_\mathrm{i} - 2\delta)}{\upsilon} \tag{18}$$

u_m being the mean flow velocity of oil in the tube, at each time t; d_i is the tube internal diameter; δ the deposit thickness; and υ the oil kinematic viscosity. The Prandtl number, Pr, is likewise defined via

$$Pr = \frac{C_\mathrm{p}\mu}{\lambda_\mathrm{c}} \tag{19}$$

C_p being the specific heat capacity, μ the dynamic viscosity and λ_c the thermal conductivity of the crude. All thermophysical properties of the crude are calculated at the local bulk oil temperature, T_b as shown in Table 1. T_b is independent of time. T_s is calculated by balancing the heat fluxes across the wall, the deposit and the tube-side heat transfer film (see Figure 2). For simplicity, the suppression term (second term on RHS in Eq. 17), which is not affected significantly by deposit ageing, is taken to be negligible. In detailed future analyses, the suppression term should be taken into account. In this study, the deposition rate is given by

$$\frac{\mathrm{d}\delta}{\mathrm{d}t} = \lambda^0_{\mathrm{f},i}\frac{\mathrm{d}R_{\mathrm{f},s}}{\mathrm{d}t} = \lambda^0_{\mathrm{f},i}\alpha Re^{-0.8}Pr^{-0.33}\exp\left(-\frac{E_\mathrm{f}}{RT_\mathrm{s}}\right) \tag{20}$$

Hence, the thickness of the ith layer is

$$\delta_i = \lambda^0_{\mathrm{f},i}\alpha Re^{-0.8}Pr^{-0.33}\exp\left(-\frac{E_\mathrm{f}}{RT_\mathrm{s}}\right)\Delta t \tag{21}$$

where T_s is the layer/oil surface temperature at time T_i, the time when layer i is deposited. Equation 21 involves several simplifications, which might require correction for particular cases: for instance, some models report the key temperature as the fluid-interface film temperature.[32]

Equations 21 and 16 are the key equations that are used to compare the combination of the deposition and the ageing process.

Modeling of Flow and Conduction

The build-up of deposit changes the hydraulic resistance to flow. In practice, two typical scenarios are used for dealing with this, namely to operate with (a) constant mass flow rate (increasing pumping power to counter higher pressure drops) and (b) constant pressure drop (reducing mass flow rate).

Fouling deposition reduces the cross-sectional area available for flow and therefore the mean tube-side velocity, u_m, changes with time. In the constant mass flow rate scenario, u_m increases with time, whereas in the constant pressure drop scenario it decreases. The surface-fluid film heat transfer coefficient also changes. The relationship between the thermal and hydraulic impacts of fouling have been discussed in detail by Yeap et al.[21]: we employ a simple relationship here. The reduction in cross-sectional area also provides a useful measure of fouling when comparing the

different ageing scenarios, as the rate of ageing ultimately affects surface temperature, fouling rate, and the thickness of the deposit formed. In all cases, we start with clean surfaces. The limit criterion chosen as termination condition for the simulations is to define a critical deposit thickness as that which would increase the pressure drop across the pipe, in the constant mass flow rate scenario, by 5%.

The pressure drop across a single, deposit-free tube, ΔP_{cl}, is given by

$$\Delta P_{cl} = 4C_f \frac{L}{d_i} \frac{\rho u_{m,cl}^2}{2} \tag{22}$$

Here, C_f is the Fanning friction factor, L the tube length, d_i the tube internal diameter, and ρ is the fluid density. The corresponding relation for a fouled tube, ΔP_f, is

$$\Delta P_f = 4C_{f,f} \frac{L}{(d_i - 2\delta)} \frac{\rho u_{m,f}^2}{2} \tag{23}$$

Assuming that deposition does not affect the surface roughness significantly and that the velocity dependence of C_f in turbulent flow can be described by the Blasius correlation ($C_f \propto \mathrm{Re}^{-0.25}$) yields

$$\Delta P_f = \Delta P_{cl} \left(1 - \frac{2\delta}{d_i}\right)^{-4.75} \tag{24}$$

The tube-side film heat transfer coefficient, h_{ts}, was calculated using the Gnielinski correlation[33]:

$$h_{is} = \left(\frac{\lambda_c}{d_i - 2\delta}\right) \frac{\left(\frac{C_f}{2}\right)(Re - 1000)Pr}{1 + 12.7\sqrt{\frac{C_f}{2}}(Pr^{0.67} - 1)} \tag{25}$$

where the value of C_f was calculated using the explicit form of the Colebrook-White correlation given by Sousa et al.[34]

$$\frac{1}{\sqrt{\frac{C_f}{2}}} = -4\log_{10}\left(\frac{e}{3.7(d_i - 2\delta)} - \frac{5.16}{Re}\log\left(\frac{e}{3.7(d_i - 2\delta)} - \frac{5.09}{Re^{0.87}}\right)\right) \tag{26}$$

with an e value of 43 μm.[17]

The derivation of the non-trivial equations of Table 2 is now complete.

As the above phenomena are closely coupled, the governing equations must be solved together. Table 2 describes the calculation sequence in the time-discretized model, starting from a clean tube.

Numerical simulations were performed on a desktop PC [AMD Athlon 64 Processor 3800+ 2.41 GHz, 2 GB of RAM] using code written in Matlab.

Impact on Local Measurements

Relative rates of deposition and ageing

The deposition rate model parameters α and E_f determine the layer thickness and the initial thermal resistance of that layer. The ageing model parameters A and E_a determine the subsequent change in the layer thermal conductivity, and the two phenomena together determine the surface temperature and subsequent rate of deposition, and ageing in all layers. Deposition and ageing therefore interact, with a ratio of characteristic frequency factors, $\psi = A/\alpha'$, where $\alpha' = \alpha\, Re^{-0.8}\, Pr^{-0.33}$ and temperature dependencies related to the difference in activation energies, $\Delta E = E_f - E_a$.

The impact of different magnitudes of parameters ψ and ΔE is investigated in the following sections, based on realistic values observed for overall measurements of crude oil fouling. The operating parameters in Table 1 represent typical conditions for a refinery preheat train exchanger and crude oil.

For a typical crude oil refinery application, activation energies for chemical reaction fouling, E_f, for the temperature range 150 to 300°C have been reported to lie in the range $20 \le E_f \le 80$ kJ mol^{-1}.[21] Schwaab and Pinto[35] and Bennett et al.[36] have reported two different approaches to assess the interrelationship of the values of pre-exponential factor and activation energy derived from the fitting of experimental data. These issues should be considered when experimental data are analyzed, requiring perhaps reparameterization of the Arrhenius equation. In this article, however, values reported by Yeap et al.[21] are used. For this range, the argument of the exponential in Eq. 17 will lie between

$$\frac{20,000}{8.3145 \times 573} \le \frac{E_f}{RT_s} \le \frac{80,000}{8.3145 \times 423}$$

$$\text{i.e.,}\ 4.2 \le \frac{E_f}{RT_s} \le 22.7 \tag{27}$$

indicating quite strong temperature dependency. For an E_f value of 50 kJ mol^{-1} and crude temperature of 190°C, $|E_f/RT_s| \sim 13$. At higher temperatures (associated with furnaces, etc.), two-phase flow behavior and coking (caused by different chemical reactions) are instead likely to dominate.

Modes of operations

We consider here the effect of ageing on fouling data collected under uniform conditions, reflecting laboratory experiments where temperature measurements are taken at a single point, or the less common case where surface conditions are uniform over a certain tube length (which may be a reasonable approximation for parts of a boiler or fired heater). We consider the case where fouling occurs on the inner surface of a tube, through which the oil flows at a (time-varying) mean tube-side velocity u_m. We note that several fouling test systems employ annular configurations, with a heated inner tube[37,38]: the analysis here can be readily extended to that geometry, particularly if the liquid flow is in the turbulent regime. Results are presented for the two main operating modes, namely (a) constant wall temperature on the nonfouling side and (b) constant heat flux. All simulations were performed taking the crude inlet temperature as 190 °C.

Constant wall temperature

In this idealized case, the temperature of the shell-side fluid remains constant and the resistances to heat transfer of

Table 1. Operating Parameters Used in the Simulations

Parameter	Value	Source
d_i	0.0229 m	Sinnott[31]
d_o	0.0254 m (tube size 1 in., Gauge 18)	
m	0.3 kg/s	Unpublished data from a UK refinery
Specific heat capacity (J kg^{-1} K^{-1})	$C_p = 1787.5 + 5.04337T_b$	
Density (kg m^{-3})	$\rho = 877.02 - 0.8379T_b$	
Dynamic viscosity (mPa s)	$\mu = 1498.7T_b^{-1.5611}$	
Thermal conductivity (W m^{-1}K^{-1})	$\lambda_c = 0.1367 - 0.00009T_b$	

T_b is the crude bulk temperature in °C.

the wall and on the shell-side are negligible so that the inner wall temperature also remains constant. Fouling reduces the rate of heat transfer, so the fluid-deposit interface temperature, T_s, will therefore decrease over time. The wall temperature in a shell-and-tube exchanger will actually vary with time due to (a) internal variations, e.g., the evolving distribution of fouling resistance and flow patterns elsewhere in the exchanger and (b) external changes such as flow rates and inlet temperatures being set by control actions, plant operation, and fouling in other units. The latter changes, in particular, are rarely systematic and can vary widely over the time taken to build up significant fouling deposits. We employ the constant wall temperature mode as an illustrative limiting case.

Base case—deposition with no ageing

First, the effects of the two operating scenarios, namely (a) constant mass flow rate and (b) constant pressure drop, are compared for a base case where no ageing occurs. Figure 3 shows the profiles of deposit thickness (and therefore fouling resistance, via Eq. 2) over a 1000 day horizon for values of $Re = 40{,}100$, $Pr = 9.5$, and $\alpha = 1 \times 10^5$m^{2}K kW^{-1} h^{-1} (low fouling rate, 4.24×10^{-11} m^2 K J^{-1}), and 1×10^6 m^{2}K kW^{-1} h^{-1} (high fouling rate, 4.24×10^{-10} m^{2}K J^{-1}). These are typical of the range reported in experimental studies. The profiles exhibit autoretardation due to the decrease in surface temperature as deposit builds up. There is little difference between the two operating scenarios for the lower fouling rate (Figure 3a) because from Eq. 24 the 0.14 mm change in deposit thickness for a tube with internal diameter 0.0229 m corresponds to a 5% reduction in cross sectional area, which is insufficient to cause a noticeable difference in flow rates for the constant pressure drop scenario.

The scenarios do deviate, discernibly but modestly, in the higher fouling rate case (Figure 3b), with the rate and extent of fouling being greater for the constant pressure drop scenario. This follows from the effect of fouling on the flow rate: with constant mass flow rate, the velocity in the duct increases inversely with change in cross section, increasing the Reynolds number, and film heat transfer coefficient, thereby reducing the surface temperature (and fouling rate). With constant pressure drop, the change in velocity is smaller, and the surface temperature does not decrease as rapidly. The deviation between the two scenarios is small and the constant mass flow rate scenario is pursued below.

The following analyses employ the lower fouling rate ($\alpha = 1 \times 10^5$ m^{2}K kW^{-1} h^{-1}) over a timescale of 250 days, where the differences between the two operating scenarios are small. Constant mass flow rates are used, replicating the operating scenario adopted in most laboratory experiments.

Deposition with ageing

The impact of ageing is now considered. In the following illustrative cases, the fouling model activation energy, E_f, is kept constant, at 50 kJ mol^{-1}, and the effect of changing E_a and the ratio of frequency factors are considered.

The initial value of α' is fixed to $\alpha Re^{-0.8}\ Pr^{-0.33}$ (in this example, 9.86 m^{2}K kW^{-1}h^{-1}) and the ratio of frequency factors, ψ, is set (arbitrarily) to 0.1, 1.0, and 10, which are termed slow, medium, and fast ageing, respectively. For each ratio, the effect of temperature sensitivity is explored by comparing E_a values of 10 kJ mol^{-1} ($\Delta E > 0$), 50 kJ mol^{-1} ($\Delta E \sim 0$), and 200 kJ mol^{-1} ($\Delta E < 0$). To provide a consistent basis for comparison, the initial ageing rate was held constant by compensating A for the change in E_a via

$$A_{Ea} = A_{10\ \mathrm{kJ/mol}} \exp\left(-\frac{10{,}000 - E_a}{RT_{wall}}\right) \tag{28}$$

If such compensation had not been introduced, the effect of increasing E_a alone would merely have been to slow the ageing rate: by contrast we wish to study the effect of increasing sensitivity of ageing rate to temperature.

The wall temperature was set at 270°C, being representative of a wall temperature at the hot end of a typical crude oil refinery preheat train (and $|E_f/RT_s| \sim 11$).

Figure 4 shows the deposit thickness and overall fouling resistance profiles over time for the different ageing rates. The base case (no ageing, shown in bold) is included on each plot for comparison. The effect of ageing is to reduce the thermal resistance of the deposit and therefore raise the deposit/crude interface temperature, promoting deposition. The final deposit thickness in Figure 4c (fast ageing) is therefore noticeably larger than the base case, or the slow ageing case in Figure 4a. All cases yield larger deposit thicknesses than the base case.

The fouling resistance plots in Figure 4b(ii) all show that the effect of ageing is to increase the degree of autoretardation over that observed in the base case. The fast ageing case (Figure 4c) shows limiting case behavior, in that the fouling resistance-time profile is almost linear. In this case, the deposit is rapidly converted to the higher thermal conductivity (coke) form, with conductivity an order of magnitude greater than that of flowing oil. The dominant resistance to heat transfer remains that of the fluid and the deposit surface temperature remains close to that of the wall, such that the rate of fouling does not change. Ageing therefore results in a change in observed thermal fouling behavior.

Ageing will clearly affect the relationship between the thermal and hydraulic effects of fouling. For fast ageing (Figure 4c), both the fouling resistance and the deposit

Table 2. Calculation Sequence for Evaluation of Layer Thermal Conductivity with Time in the Time-Discretised Model

Step	Equation
1. Initialization. At $t_0 = 0$, clean surface, *i.e.*, $i = 1$, $\delta = 0$, $n = 0$ (here subscript i indicates the ith layer and subscript n indicates the nth time instance.)	
2. Formation of new layer: $t_{n+1} = t_n + \Delta t$ and $n = n + 1$	$\frac{d\delta}{dt} = \lambda_f^0 \frac{dR_{f,s}}{dt}$, Eq. 20
	$\delta_n = \lambda_f^0 \alpha Re^{-0.8} Pr^{-0.33} \exp\left(-\frac{E_f}{RT_s}\right)\Delta t$, Eq. 21
	$\lambda_{f,i=n}^{t_n} = \lambda_f^0$
3. Calculate thermal resistance of each layer, $\delta_i/\lambda_{f,i}^{t_{n-1}}$, and total deposit thermal thermal resistance	$R_f = \sum_{i=1}^{n} \frac{\delta_i}{\lambda_{f,i}^{t_{n-1}}}$, Eq. 5
4. Calculate h_{ts} and U	$h_{is} = \left(\frac{\lambda_c}{d_i - 2\delta}\right) \frac{\left(\frac{C_f}{2}\right)(Re - 1000)Pr}{1 + 12.7\sqrt{\frac{C_f}{2}}(Pr^{0.67} - 1)}$, Eq. 25
	$\frac{1}{U} = \frac{1}{h_{ts}} + R_f$, Eq. 1
5. Calculate teat flux (T_{wall} constant) or T_{wall} (q constant)	$q = U(T_{wall} - T_{bulk})$
	$T_{wall} = T_{bulk} + q/U$
6. Calculate layer temperatures and T_s	Solve coupled simultaneous equations for thermal conduction of each layer based on $q = \frac{\lambda_{f,i}^{t_{n-1}}(T_{i-1} - T_i)}{r \ln\left(\frac{d_i - 2\sum_{j=1}^{i-1}\delta_j}{d_i - 2\sum_{j=1}^{i}\delta_j}\right)}$ where $i > 1$ q is the heat flux at a given radius r
7. Update $\lambda_i^{t_{n-1}} (i = 1, \ldots, n)$	$\Delta \ln y_i^{t_{n-1}} = \left[-A \exp\left(\frac{-E_a}{RT_{i,d}}\right)\right]\Delta t$, Eq. 12
8. Update layer thermal conductivities $\lambda_i^{t_{n-1}} (i = 1, \ldots, n-1)$	$\lambda_{f,i}^{t_{n-1}} = \lambda_{f,i}^{\infty} + \left[\lambda_{f,i}^0 - \lambda_{f,i}^{\infty}\right] y_i^{t_{n-1}}$ Eq. 7
9. Report	
10. Terminate when δ reach the critical deposit thickness (here, deposit thickness to increase pressure drop by 5% as in Eq. 24). Otherwise move to the next layer, step 2	

thickness increase almost linearly with time, so the effects of fouling on pressure drop and heat transfer will be related in a simple manner. With slow ageing (Figure 4a), the two effects have a close initial correlation, but later in time the change in pressure drop is not matched by a change in thermal performance. Deposit ageing could cause a heat exchanger to reach a hydraulic limit considerably earlier than it would reach its thermal limit.

In the constant wall temperature mode, the heat flux decreases steadily as deposit builds up and the temperature in the deposit always lies within the range $T_b \leq T_i \leq T_{wall}$. The Arrhenius-type dependency in the ageing rate model (Eq. 11) means that a high E_a process will be very sensitive to this change in temperature, and ageing will slow rapidly once the deposit develops. This is evident in all the Figure 4 profiles, where the $E_a = 200$ kJ mol^{-1} responses lie closest to the no-ageing base case (corresponding to $E_a = \infty$). As the ratio of pre-exponential factors increases (i.e., faster ageing, Figure 4c) the effect of E_a is reduced as the deposit is converted to the higher conductivity form more rapidly, and ultimately the rate of ageing is so fast that the material is converted to the higher conductivity form soon after being formed, so there is little effect of E_a. The difference between the profiles is arguably greatest for the medium case (Figure 4b), with the R_f–t behavior changing from pseudo-asymptotic for $E_a = 200$ kJ mol^{-1} to pseudo-linear for $E_a = 10$ kJ mol^{-1}.

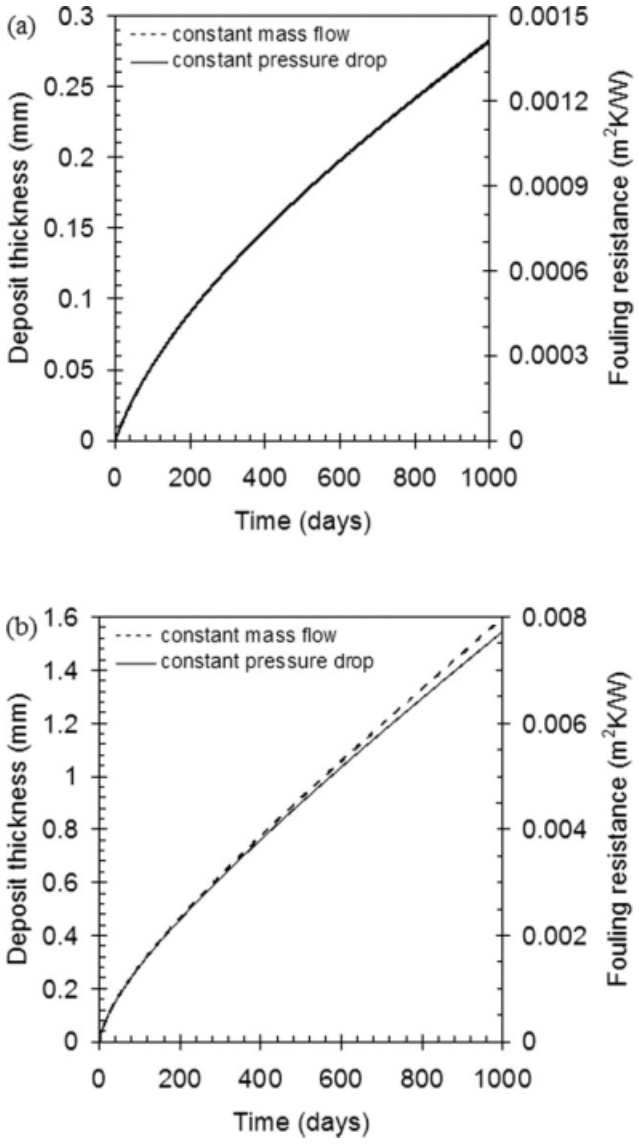

Figure 3. Fouling behaviour for constant mass flow rate (dashes loci) and constant pressure drop (solid loci) scenarios, T_{wall} constant.

(a) $\alpha = 1 \times 10^5$ m^{2}K kW^{-1} h^{-1} (b) $\alpha = 1 \times 10^6$ m^{2}K kW^{-1} h^{-1}.

The evolution of the state of the deposit layer formed next to the heat transfer surface (i.e., the wall layer) is presented in Figure 5. The initial wall temperature is 270°C; this drops immediately once the first deposit is formed. Over time, the temperature climbs back towards T_{wall}, and the thermal conductivity increases. In the slow ageing case (Figure 5a), this oldest layer of deposit does not reach the upper limit of thermal conductivity over the timescale of these simulations, whereas it is reached for some cases in Figure 5b. In the limit of fast ageing, Figure 5c, all cases show the transition between the lower and upper limits of thermal conductivity (0.2 and 1 W m^{-1} K^{-1}) and the path is independent of E_a over the range of values considered.

These results illustrate that if the deposit does undergo ageing, calculations which neglect ageing will over-predict the thermal effect of fouling. Conversely, thermal resistance data collected over a long period of time, such that ageing can have occurred, will underestimate the deposit thickness and pressure drop. The hydraulic effect, which is related to deposit thickness, may be noticed before the change in thermal performance becomes important.

Constant heat flux (constant mass flow rate)

Experiments are often performed under conditions of constant heat flux. If the film heat transfer coefficient does not change over time, the deposit surface temperature will remain constant and linear fouling will be observed (e.g., Eq. 17) rather than the decreasing rate profiles obtained earlier. Deposition is therefore accelerated, but ageing is also affected: the heat flux, q, is related to the temperature difference across the deposit by the overall fouling resistance via

$$q = h_i(T_s - T_b) = \frac{1}{R_f}(T_{wall} - T_s) \tag{29}$$

Maintaining q, h_i, and T_b constant forces T_s to be constant. At the start of a test, when no deposit is present, $T^0_{wall} = T_s$. It follows that

$$T_{wall} = T_s + R_f q \tag{30}$$

Thus, the temperature within the deposit increases steadily over time, and ageing, as described by the kinetic model presented here, will be accelerated. Equation 30 can also be written as

$$\begin{aligned} T_{wall} - T_s &= Bi_f(T_s - T_b) \\ \frac{T_{wall} - T_s}{T_s - T_b} &= Bi_f \end{aligned} \tag{31}$$

reinforcing the impact of fouling on temperatures in the deposit.

We illustrate this with simulations similar to those in the previous section but with a constant heat flux supplied at the tube outer surface. The value of q was selected to give the same initial surface temperature (270°C) as in the constant wall temperature mode. The calculation method is similar to before, but with a change in sequence in step 5 in Table 1.

Simulations were performed with $\alpha = 1 \times 10^5$ m^{2}K kW^{-1} h^{-1}. The nonageing results in Figure 6 illustrate how constant heat flux operation (without ageing) yields a linear deposit thickness-time profile and a final fouling resistance ~1.7 times greater (in this case) than constant T_{wall} operation after 250 days. In this case, the deposit thickness after 250 days for the constant heat flux operation is 180 μm, which is negligible compared with the tube internal diameter of 0.0229 m. Hence, the effect on pressure drop is not significant.

Figure 7 presents the $R_f - t$ profiles for simulations of the slow, medium, and fast ageing cases with the same E_a values and compensated pre-exponential factors as before. The base case (no ageing) is included for comparison. Profiles showing autoretardation are evident in the slow ageing case (Figure 7a)—even though the deposit thickness is increasing

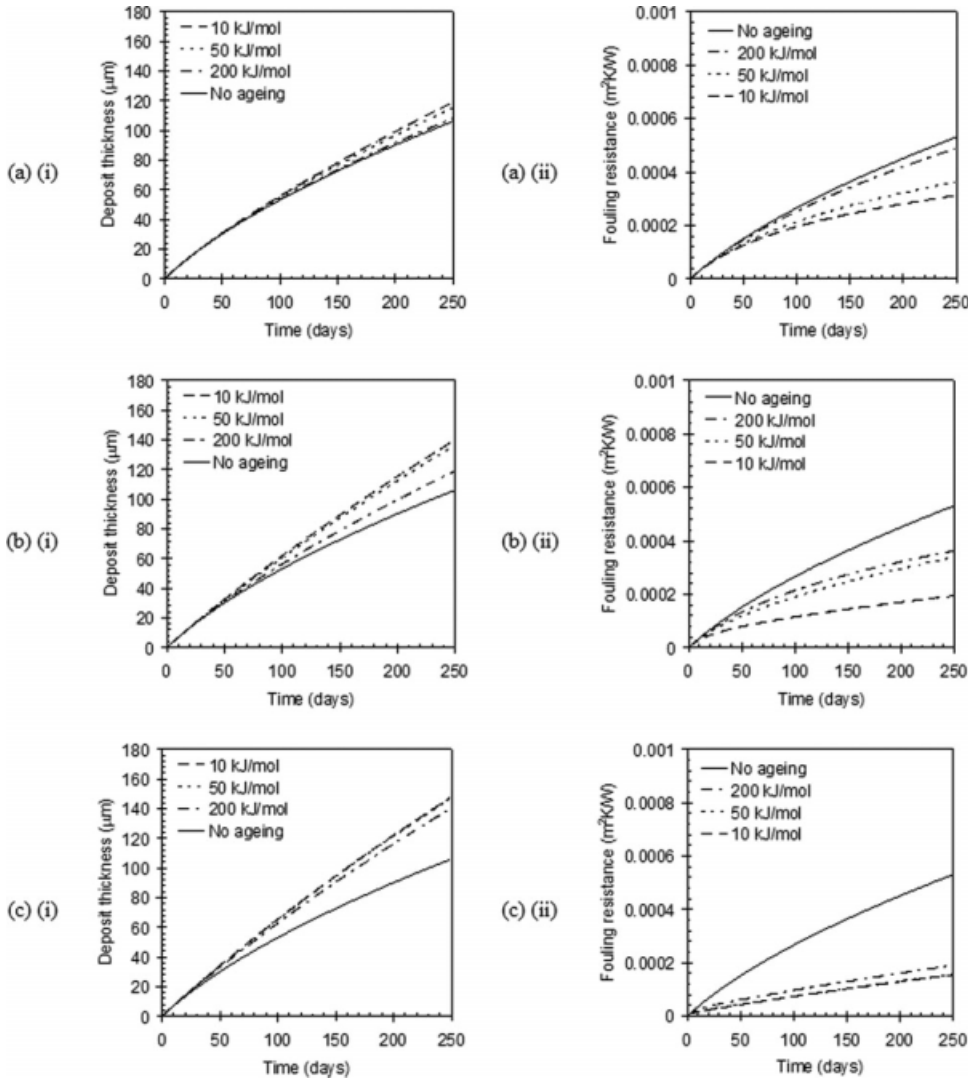

Figure 4. Effect of ageing on fouling behavior, constant T_{wall} operation.

(i) Deposit thickness and (ii) overall fouling resistance. Relative rate of ageing: (a) slow, (b) medium, and (c) fast.

linearly—in a manner similar to the constant T_{wall} case. The other cases, however, exhibit linear fouling characteristics. With fast ageing (Figure 7c), formation of the high thermal conductivity material is almost instantaneous (plotted in Figure 8c) and the R_f value after 250 days is ~1/5th that of the nonageing case, which would be expected from the ratio $\lambda^0_{f,i}/\lambda^\infty_{f,i} = 0.2$. This illustrates the experimental problem posed by ageing in accelerated tests, i.e., the deposit recovered after a test may not reflect the form of the original precursor, thereby disguising the true fouling mechanism. In the limit, the fast ageing case is similar to the classical view of chemical reaction fouling, whereby a precursor is transported to the surface and forms deposit, except that in this case the deposit consists of aged material.

The 'measured' fouling rate, extracted from the gradient of the $R_f - t$ profile in Figure 7c), will therefore be a factor of 5 smaller than the true deposition rate (represented by the base case). The 'rate' extracted from Figure 7b will also be low, but to a lesser degree owing to the reduced extent of ageing (presented in Figure 8b). According to Figure 6, however, both the aged and the non-aged deposit have almost the same deposit thickness; the fouling resistance values calculated from temperature measurements would mask the actual degree of deposit formation causing misinterpretation of the degree of fouling.

One important difference between constant heat flux and constant wall temperature operation here is that the deviation from base case behavior due to ageing is greatest for the high E_a case. The deposit temperatures are always greater than the initial value, so the enhanced temperature sensitivity results in faster ageing, as demonstrated by the evolution of first layer thermal conductivity in Figure 8a. The wall layer temperature profiles differ noticeably with E_{act}, by over 100 K. The absolute value of wall temperature should not be interpreted closely in terms of chemistry, as the calculations are illustrative: the values given are relatively low for coking processes (~550°C[23]). Increasing the rate of ageing (Figure 8b-c) causes a rapid approach to the upper thermal

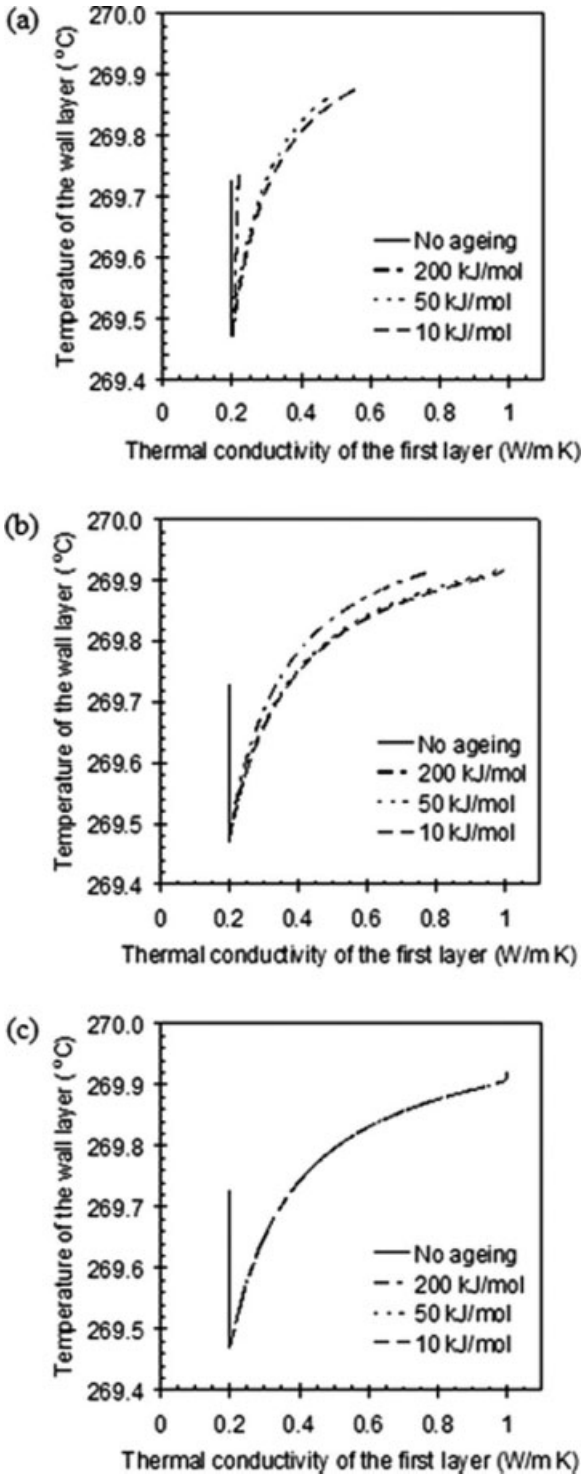

Figure 5. Evolution of average temperature and thermal conductivity of deposit layer next to the wall, constant T_{wall} operation (as Figure 4).

(a) slow, (b) medium, and (c) fast ageing.

conductivity limit, with progressively less sensitivity to E_a. Ageing must therefore be considered when interpreting data obtained from accelerated tests: the results from Figure 7b,c could not be applied with confidence to the constant wall temperature mode.

The models presented do represent typical behavior actually observed, but would clearly benefit from experimental validation. Experimental reports of ageing in crude oil systems are however sparse. Asomaning et al.[39] mentioned, briefly, observations of linear and asymptotic $R_f - t$ behavior as a result of ageing. They suggested that the accelerated fouling conditions often employed in laboratory tests may give rise to rapid ageing of deposits and that this ageing could result in a reduction in deposit strength due to rapid thermal degradation, facilitating removal and potentially giving the appearance of asymptotic fouling behavior. Polymerization, however, can serve to strengthen deposits. There is therefore a need for careful experimental investigations.

Conclusions

A kinetic model for deposit ageing has been proposed as suitable for exploratory calculations. It is based on simple chemical principles, namely first order kinetics, Arrhenius temperature behavior and the effective media theory model (see Appendix B) for the conductivity of a two-phase mutually dispersed material. The model has been coupled with heat transfer and solutions obtained using a simple numerical scheme. Simulations were performed representing laboratory-scale point fouling measurements, under conditions representative of tube-side fouling in the preheat train heat exchangers in a crude oil refinery. Two operating modes, namely (a) constant tube-wall temperature and (b) constant heat flux, were investigated.

When the tube wall temperature is held constant, ageing increases the rate of deposit build-up but reduces the thermal effect of the fouling layer. This difference becomes more noticeable as the rate of ageing increases, particularly when the ageing mechanism is not very sensitive to temperature. The simulations also show that ageing changes the relationship between the hydraulic and thermal impacts of fouling.

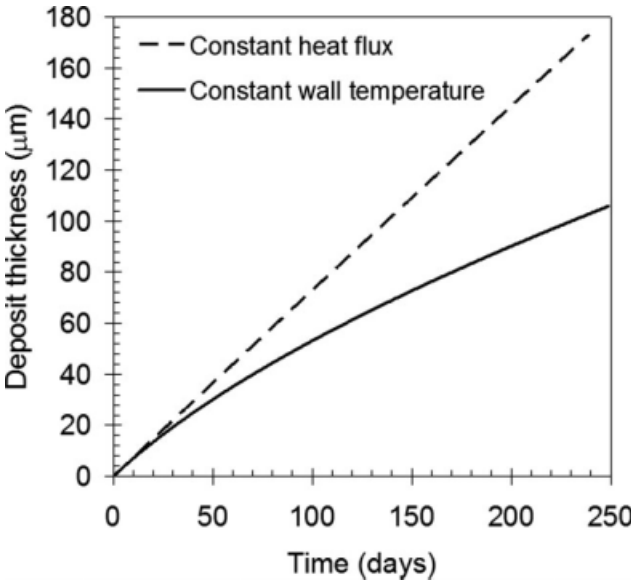

Figure 6. Comparison of deposition behavior for constant T_{wall} (solid locus, reproduced from Figure 3) and constant heat flux operation (dashed locus), in the absence of ageing.

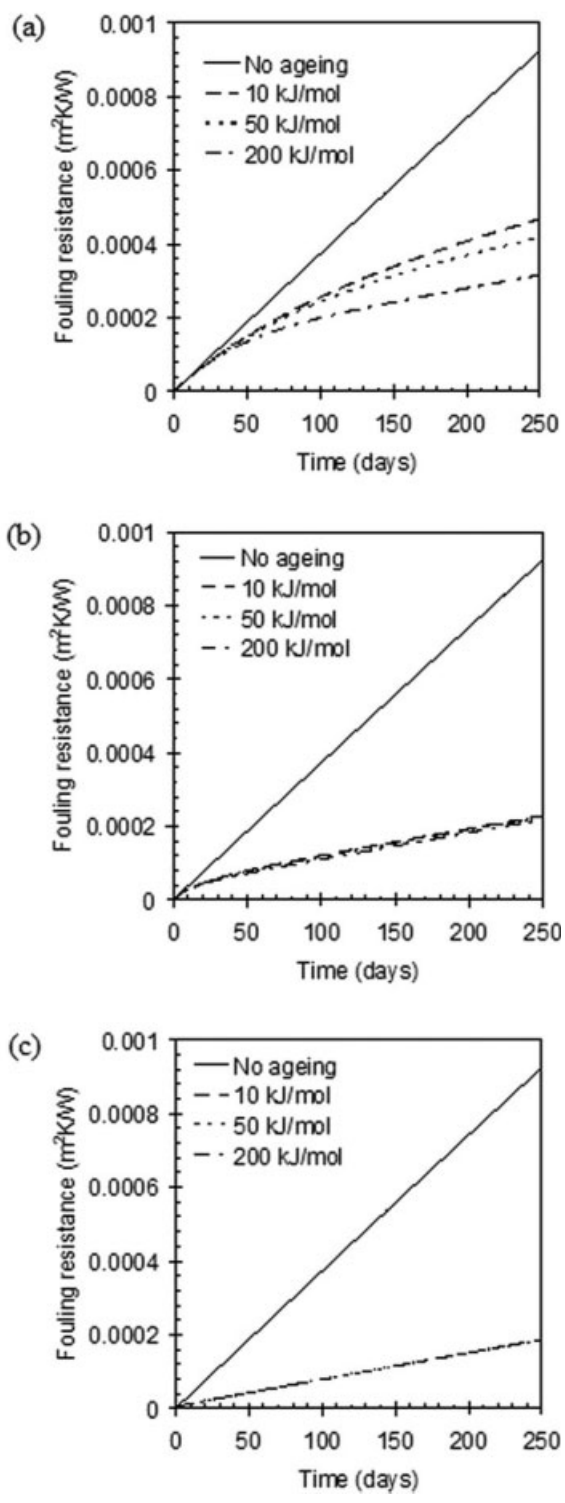

Figure 7. Effect of ageing on thermal fouling behavior.

Constant heat flux operation; relative rate of fouling: (a) slow, (b) medium, and (c) fast.

When experiments are performed under conditions of constant heat flux, modeling predicts that the behavior observed is determined by the relative rate of ageing to the rate of deposition. Relatively slow ageing gives rise to autoretardative thermal fouling behavior, whereas faster ageing yields pseudo-linear thermal fouling but at a rate different from that which would be obtained in the absence of ageing. Operating in the constant heat flux mode causes a

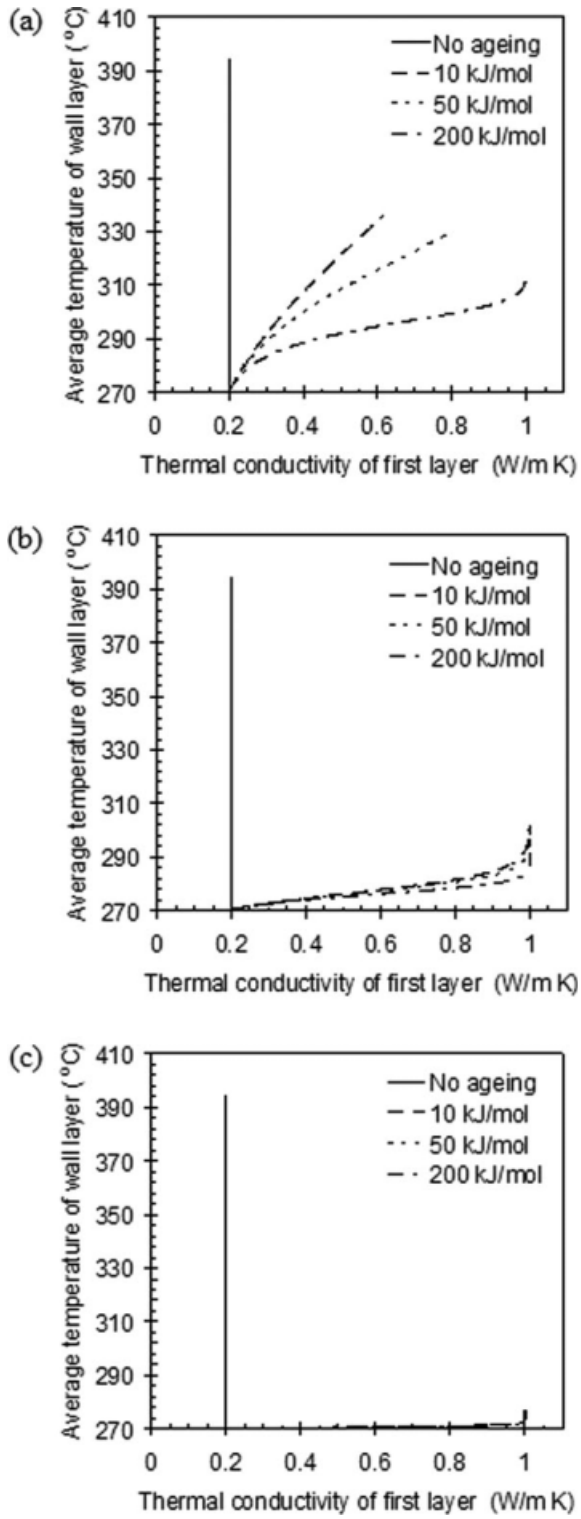

Figure 8. Evolution of average temperature and thermal conductivity of deposit layer next to the wall, constant heat flux operation (as Figure 7).

(a) slow, (b) medium, and (c) fast ageing.

progressive increase in temperature within the deposit and the rate of ageing is therefore greatest for a highly temperature-sensitive ageing step. The analysis illustrates how ageing in accelerated fouling tests can cause problems in interpreting experimental data and translating the results to constant wall temperature systems, which are more representative of operating heat exchangers. It also shows that fouling ageing dynamics should indeed be incorporated in models which aim at describing heat exchanger behavior over medium-long times (a few weeks to a few years) for the purpose of improving process operations or equipment design.

Acknowledgments

Funding from EPSRC projects EP/D50306X/1 and EP/D503051/1 as well as financial support for EMI from the Cambridge Overseas Trust is gratefully acknowledged.

Notation

a = constant in Eq. B1
a' = constant in Eq. B3, W m^{-1} K^{-1}
A = frequency factor of the ageing model, day^{-1}
A^* = group of parameters, Eq. 14, W K^{-1} s^{-1}
b = constant in Eq. B1
b' = constant in Eq. B3, W m^{-1} K^{-1}
Bi_f = fouling Biot number
c = constant in Eq. B1, day^{-1}
C_f = Fanning friction factor
C_p = specific heat capacity, J kg^{-1} K^{-1}
d = tube diameter, m
e = surface roughness, m
E_a = activation energy for ageing model, J mol^{-1}
E_f = activation energy for fouling rate, J mol^{-1}
h = heat transfer coefficient, W m^{-2} K^{-1}
k = ageing rate constant, day^{-1}
L = tube length, m
m = mass flow rate, kg s^{-1}
n = number of layers
q = heat flux, W m^{-2}
Pr = Prandtl number
r = radius, m
R = gas constant, J mol^{-1} K^{-1}
R_f = fouling resistance, m^2 K W^{-1}
Re = Reynolds number
t = time, s
T = temperature, K
u_m = mean flow velocity, m s^{-1}
U = overall heat transfer coefficient, W m^{-2} K^{-1}
V_i = volume of component i, cm^3
v_i = volume fraction of component i
w_i = mass of component i, kg
X = lumped variable in Eq. 16, m K W^{-1}
y = youth function
z = distance from the tube outer surface, m

Subscripts

b = bulk
$cl_{coke\ =\ coke\ layer}$ = clean state
d = deposit
Ea = activation energy for ageing model
f = fouled state
i = ith layer, internal
o = external/outer
s = surface
tar = tar layer
ts = tubeside
wall = wall

Superscripts

0 = initial state
∞ = final state
t = time instant t
* = lumped state

Greek letters

α = constants in fouling models, m^{2}K kW^{-1} h^{-1}
γ = constants in fouling models, m^{2}K kW^{-1} h^{-1}
δ = thickness of the foulant layer, m
ΔH_f = H_f enthalpy of formation, J mol^{-1}
ΔP = pressure drop, Pa
Δt = time gap, s
ΔE = difference between the activation energies ($E_a - E_f$), J mol^{-1}
ϕ = H/C atomic ratio, –
ψ = ratio of the frequency factors, –
λ_i = thermal conductivity of phase i
λ_c = thermal conductivity of the crude, W m^{-1} K^{-1}
λ_e = equivalent thermal conductivity, W m^{-1} K^{-1}
λ_f = thermal conductivity of the foulant material, W m^{-1} K^{-1}
λ_j = thermal conductivity of material j, W m^{-1} K^{-1}
μ = dynamic viscosity, kg m^{-1} s^{-1}
ρ = density, kg m^{-3}
υ = kinematic viscosity, m^2 s^{-1}

Literature Cited

1. Taborek J, Aoki T, Ritter RB, Palen JW, Knudsen JG. Fouling—the major unresolved problem in heat transfer. *Chem Eng Prog*. 1972; 68:59–67.
2. ESDU. Heat exchanger fouling in the preheat train of a crude oil distillation unit. Data Item 00016. London, UK: IHS-ESDU International plc, 2000:5.
3. Epstein N. Thinking about heat transfer fouling: a 5×5 matrix. *Heat Transfer Eng*. 1983;4:43–56.
4. Watkinson AP, Wilson DI. Chemical reaction fouling: a review. *Exp Thermal Fluid Sci*. 1997;14:361–374.
5. Chew JYM, Paterson WR, Wilson DI. Fluid dynamic gauging for measuring the strength of soft deposits. *J Food Eng*. 2004;65:175–187.
6. Nelson WL. Fouling of heat exchangers. *Refiner Nat Gas Manufacturer*. 1934;13:271–276, 292–298.
7. Atkins GT. What to do about high coking rates. *Pet/Chem Eng*. 1962;34:20–25.
8. Crittenden BD, Kolaczkowski ST. *Energy savings through the accurate prediction of heat transfer fouling resistances*. In: O'Callaghan PW, editor. *Energy for Industry*. Oxford: Pergamon Press, 1979:257–266.
9. Watkinson AP, Epstein N. Gas oil fouling in a sensible heat exchanger. *Chem Eng Prog Symp Ser*. 1969;65:84–90.
10. Bohnet N, Augustin W, Hirsch H. *Influence of fouling layer shear strength on removal*. In: Bott TR, Melo LF, Panchal CB, Somerscales EFC, editors. *Understanding Heat Exchanger Fouling and Its Mitigation*. New York: Begell House, 1999:201–208.
11. Singh P, Venkatesan R, Fogler HS. Formation and aging of incipient thin film wax-oil gels. *AIChE J*. 2000;46:1059–1074.
12. Singh P, Venkatesan R, Fogler HS. Morphological evolution of thick wax deposits during aging. *AIChE J*. 2001;47:6–18.
13. Singh P, Youyen A, Fogler HS. Existence of a critical carbon number in the aging of a wax-oil gel. *AIChE J*. 2001;49:2111–2124.
14. Paso KG, Fogler HS. Influence of *n*-paraffin composition on the aging of wax-oil gel deposits. *AIChE J*. 2003;49:3241–3252.
15. Paso KG, Fogler HS. Bulk stabilization in wax deposition systems. *Energy Fuels*. 2004;18:1005–1013.
16. Watkinson AP. Critical review of organic fluid fouling. *Final Report, ANL/CNSV-TN-208*. Argonne National Laboratory: US Department of Energy, 1988:136.
17. Perry RH, Green DW. *Perry's Chemical Engineers' Handbook*, 7th ed. New York: McGraw-Hill, 1997:6–10.
18. Kern DQ. *Process Heat Transfer*. Singapore:McGraw-Hill, 1988:796.
19. Jeronimo MAS, Melo LF, Braga AS, Ferreira PJDF, Martins C. Monitoring the thermal efficiency of fouled heat exchangers: a simplified method. *Exp Thermal Fluid Sci*. 1997;14:455–463.

20. Takemoto T, Crittenden BC, Kolaczkowski ST. Interpretation of fouling data in industrial shell and tube heat exchangers. *Chem Eng Res Des*. 1999;77:769–778.
21. Yeap BL, Wilson DI, Polley GT, Pugh SJ. Mitigation of crude oil refinery heat exchanger fouling through retrofits based on thermo-hydraulic fouling models. *Chem Eng Res Des*. 2004;82:53–71.
22. Polley GT, Wilson DI, Yeap BL, Pugh SJ. Evaluation of laboratory crude oil threshold fouling data for application to refinery pre-heat trains. *Appl Thermal Eng*. 2002;22:777–788.
23. Fan Z, Watkinson P. Aging of carbonaceous deposits from heavy hydrocarbon vapors. *Ind Eng Chem Res*. 2006;45:6104–6110.
24. Fan Z, Watkinson P. Formation and aging of deposits from coker vapours. In: *Proceedings of 9th Annual International Conference on Petroleum Phase Behaviour and Fouling*, Victoria, British Columbia, Canada, 2008.
25. Atkins PW. *The Elements of Physical Chemistry*, 3rd ed. Oxford: Oxford University Press, 2003:234.
26. Taylor WF, Wallace TJ. Kinetics of deposit formation from hydrocarbon fuels at high temperatures: general features of the process. *Ind Eng Chem Prod Res Dev*. 1967;6:258–262.
27. Taylor WF, Wallace TJ. Kinetics of deposit formation from hydrocarbons: effect of trace surface compounds. *Ind Eng Chem Prod Res Dev*. 1968;7:198–202.
28. Taylor WF. Kinetics of deposit formation from hydrocarbons: fuel composition studies. *Ind Eng Chem Prod Res Dev*. 1969;8:375–380.
29. Bender P, Farber J. The heats of combustion of anthracene transannular peroxide and dianthracene. *J Am Chem Soc*. 1952;74;1450–1452.
30. Westrum EF, Wong S. Strain energies and thermal properties of globular and polynuclear aromatic molecules. *AEC Rept. Coo-1149–92 Contract AT(11–1)-1149*. 1967:1–7.
31. Sinnott RK. *Coulson & Richardson's Chemical Engineering*, *Vol*. 6, 3rd ed. Oxford: Butterworth-Heinemann. 1999:634–668.
32. Ebert W, Panchal CB. *Analysis of Exxon crude-oil-slip stream coking data*. In: Panchal CB, Bott TR, Sommerscales EFC, Toyama S, editors. *Fouling Mitigation of Industrial Heat-Exchange Equipment*. New York: Begell House, 1997:451–460.
33. Gnielinski V. New equations for heat and mass-transfer in turbulent pipe and channel flow. *Int Chem Eng*. 1976;16:359–368.
34. Sousa J, Conceição M da, Marques A Sá. An explicit solution to the Colebrook-White equation through simulated annealing. In: Savic DA, Walters GA, editors. *Water Industry Systems: Modelling and Optimization Applications*, *vol*. 2. Baldock, Hertfordshire: Research Studies Press Ltd., 1999:347–355.
35. Schwaab M, Pinto JC. Optimum reference temperature for reparameterization of the Arrhehenius equation. Part 1. Problems involving one kinetic constant. *Chem Eng Sci*. 2007;62:2750–2764.
36. Bennett CA, Kistler RS, Nangia K, Al-Ghawas W, Al-Hajji N, Al-Jemaz A. Observation of and isokinetic temperature and compensation effect for high temperature crude oil fouling. In: *Proceedings of 7th International Conference on Heat Exchanger Fouling and Cleaning*, Tomar, Portugal, 2007.
37. Asomaning S. The role of olefins in fouling of heat exchangers, *Master of Applied Science Thesis*. British Columbia: University of British Columbia, 1990:65–67.
38. Watkinson AP. Deposition from crude oils in heat exchangers. *Heat Transfer Eng*. 2007;28:177–184.
39. Asomaning S, Panchal CB, Liao CF. Correlating field and laboratory data for crude oil fouling. *Heat Transfer Eng*. 2000;21:17–23.
40. Godman BT. Thermodynamic property prediction for solid organic compounds based on molecular structure, *Ph.D. Dissertation*. Brigham Young University, 2003.
41. Wang J, Carson JK, North MF, Cleland DJ. A new structural model of effective thermal conductivity for heterogeneous materials with co-continuous phases. *Int J Heat Mass Transfer*. 2008;51:2389–2397.

Appendix A: Roughness

The roughness of the surface is assumed to remain constant and is taken here to be that of the clean tube. This is a simplification as roughness effects can be significant in chemical reaction fouling (see Figure 3 in Watkinson and Wilson[4]) but is deemed appropriate here as otherwise we should need to introduce further unknown parameters. There are two main impacts of roughness on deposit ageing, namely (a) mechanical and (b) thermal. The former are those arising directly from the increase in shear stress at the deposit-flow interface, which can not only affect the fouling rate (e.g., via the suppression term) but also the structure of the deposit generated. Because the thermal conductivity of the fouling layer is determined by its microstructure, this will affect the observed fouling resistance.

The thermal effects arise from the change in heat transfer coefficient associated with surface roughness. Equation A1 presents the definition of the thermal effect of fouling (the fouling resistance) in its simplified form, *viz*.

$$\frac{1}{U} = \frac{1}{U_{\mathrm{cl}}} + R_{\mathrm{f}} \tag{A1}$$

An increase in roughness increases the deposit-fluid heat transfer coefficient, h_{s}, thereby increasing U_{cl}, so that either the value of R_{f} inferred from measurements is smaller than that obtained in the absence of changes or the observed value of U is larger. The impact on ageing will depend on the operating mode, and we here consider the case where heating the fluid causes fouling.

For the condition of a fixed temperature difference, an increase in roughness for a given thickness of fouling layer

Table A1. Relationship Between H/C Atomic Ratio and the Equivalent Thermal Conductivity of the Compound When Different Amounts of (1) Carbon Graphite and (2) Paraffin Wax are Mixed Together

w_1 (g)	w_2 (g)	No. of H atoms	No. of C atoms	H/C atomic ratio	V_1 (cm^3)	V_2 (cm^3)	v_1 (volume fraction)	v_2 (volume fraction)	λ_e (W/m K) Equally dispersed phase
100	0	0.00	8.33	0.00	60.98	0.00	1.00	0.00	4.40
90	10	1.49	8.21	0.18	54.88	10.99	0.83	0.17	3.38
80	20	2.98	8.09	0.37	48.78	21.98	0.69	0.31	2.52
70	30	4.47	7.96	0.56	42.68	32.97	0.56	0.44	1.80
60	40	5.96	7.84	0.76	36.59	43.96	0.45	0.55	1.22
50	50	7.45	7.71	0.97	30.49	54.95	0.36	0.64	0.80
40	60	8.94	7.59	1.18	24.39	65.93	0.27	0.73	0.53
30	70	10.43	7.46	1.40	18.29	76.92	0.19	0.81	0.38
20	80	11.91	7.34	1.62	12.20	87.91	0.12	0.88	0.29
10	90	13.40	7.22	1.86	6.10	98.90	0.06	0.94	0.24
0	100	14.89	7.09	2.10	0.00	109.89	0.00	1.00	0.20

w_i, the mass of component i; V_i, the volume of component i; v_i, the volume fraction of component i; and λ_e, the effective thermal conductivity of the compound calculated based on Eq. B1.

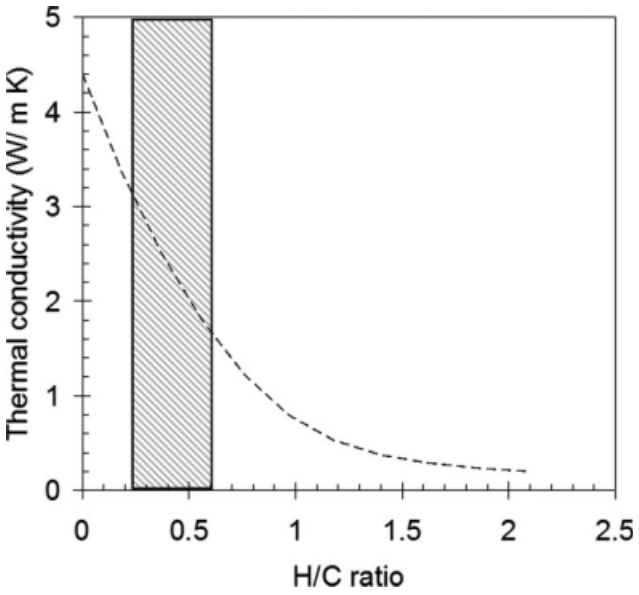

Figure A1. Compound thermal conductivity against H/C atomic ratio. Highlighted region denotes the range of H/C ratios reported in Fan and Watkinson's ageing study.[23]

results in a larger value of h_s, U, and therefore local heat flux. The increase in heat flux will not be as large as the increase in h_s, owing to the finite contribution from other resistances, so the deposit-fluid temperature will be higher than in the constant roughness case, and ageing in the deposit will therefore proceed more rapidly. The thermal resistance of the deposit layer will therefore be smaller than that of the constant roughness case, reinforcing the enhancement in heat transfer due to the change in roughness. However, these combine to give a higher deposit surface temperature and the effect on the overall fouling rate depends on the balance between temperature and suppression/shear effects.

For constant heat flux operation, the larger value of h_s will result in a lower deposit-fluid interface temperature and the temperatures across the deposit layer will therefore be lower than those in the constant roughness case. Ageing will therefore be slower than in the base case, and the thermal resistance of the fouling deposit will not decrease as quickly due to ageing. The rate of deposition, which is determined by conditions at the fluid-deposit interface, will, however, decrease as both the temperature and fluid shear effects will act to reduce the deposition rate.

Appendix B: Thermal Conductivity of Composite Layer

Published data for the thermal conductivity, λ, of solid organic compounds are relatively sparse compared to data for metals and oxides.[40] We present here an attempt to derive a relationship between λ and the H/C atomic ratio, ϕ, for solid organic mixtures which can then be related to the impact of ageing on a fouling deposit.

Fan and Watkinson reported experimental studies on coker deposits (at 550°C) where ϕ decreased from 0.6 to 0.26 over 3 days and followed a first order exponential decay of the form[23,24]

$$\phi = a + b\exp(-ct) \tag{B1}$$

where a, b, and c are positive constants and t the ageing time.

To relate ϕ to deposit thermal conductivity a model for heterogeneous materials with co-continuous phases is required. Wang et al.[41] reviewed several of the models available and recommended the following effective media theory (EMT) model for the effective thermal conductivity, λ_e, of a two-phase mutually dispersed material:

$$v_1\frac{\lambda_1-\lambda_e}{\lambda_1-2\lambda_e}+v_2\frac{\lambda_2-\lambda_e}{\lambda_2-2\lambda_e}=0 \tag{B2}$$

where v_i is the volume fraction and λ_i the thermal conductivity of phase i. Table A1 was generated for a range of graphite/paraffin wax mixtures, with λ_i values of 4.4 W m^{-1} K^{-1} for graphite and 0.2 W m^{-1} K^{-1} for paraffin wax,[16] and densities of 1.64 g/cm^3 for graphite and 0.91 g/cm^3 for paraffin wax.[17] The composition of paraffin wax was taken to be $C_{20}H_{42}$. Plotting the equivalent thermal conductivity against H/C atomic ratio shows a nonlinear relationship (Figure A1). The region where Fan and Watkinson conducted their experiments is highlighted. In this region, however, the compound thermal conductivity can be approximated as being linear in ϕ, yielding the following simple relationship:

$$\lambda_f = a' - b'\phi \tag{B3}$$

where a' and b' are positive constants. Combining Eqs. B3 and B1 yields

$$\lambda_f = a' - ab' - bb'\exp(-ct) \tag{B4}$$

which is equivalent to the form of Eq. 7 when the solution to the ODE (Eq. 9) at a given temperature is substituted,

$$\lambda_{f,i}^t = \lambda_{f,i}^\infty + \left[\lambda_{f,i}^0 - \lambda_{f,i}^\infty\right] y_0 \exp\left(-k_i^t\, t\right) \tag{B5}$$

Thus, Eq. B5 justifies adoption of Eq. 12 as a reasonable starting point to model variation in thermal conductivity with deposit ageing.

Manuscript received Jan. 12, 2009, revision received Mar. 23, 2009, and final revision received May 22, 2009.